RSC Advances

ROYAL SOCIETY OF CHEMISTRY

www.rsc.org/advances

Maltol, a Maillard reaction product, exerts anti-tumor efficacy in H22 tumor-bearing mice via improving immune function and inducing apoptosis

Wei Li [1], Xiao-min Su [1], Ye Han [1], Qi Xu [1], Jing Zhang [1], Zi Wang [1*], and Ying-ping Wang [2*]

[1] *College of Chinese Medicinal Materials, Jilin Agricultural University, Changchun 130118 China;*

[2] *Institute of Special Wild Economic Animals and Plant, CAAS, Changchun 132109, China.*

Abbreviations:

HCC	Hepatocellular carcinoma	IFN-γ	interferon-γ
IL-2	interleukin-2	TNF-α	Tumor necrosis factor-α
IL-6	interleukin-6	VEGF	Vascular endothelial growth factor

Running title: antitumor effect of maltol on H22 tumor-bearing mice

Correspondence

Professor Ying-ping Wang, Institute of Special Wild Economic Animals and Plant, CAAS, Changchun 132109, China.

E-mail: yingpingw@126.com; **Tel. /Fax**: +86-431-81919856.

Professor Zi Wang, College of Chinese Medicinal Materials, Jilin Agricultural University, Changchun 130118 China

E-mail: wangzi8020@126.com; **Tel. /Fax:** +86-0431-84533304(8011)

Abstract

The purpose of this study was to investigate the anti-hepatoma activity of maltol, a Maillard reaction product, in H22 tumor-bearing mice. The results demonstrate that maltol not only significantly inhibited the growth of hepatoma H22 transplanted in mice, but also prolonged the survival time of H22-bearing mice. Furthermore, the levels of serum cytokines in H22 tumor-bearing mice, such as interferon gamma (IFN-γ), tumor necrosis factor-α (TNF-α), interleukin-6 (IL-6), and interleukin-2 (IL-2), were enhanced by maltol treatment. Importantly, immunohistochemical and western blotting analysis clearly show that maltol treatment increased Bax and decreased Bcl-2 protein expression levels of H22 tumor tissues in a dose-dependent manner. Collectively, our findings in the present study clearly demonstrate that the maltol markedly suppressed the tumor growth of H22 transplanted tumor *in vivo* at least partly via improving the immune functions, inducing apoptosis, and inhibiting angiogenesis.

Key words: Maltol; Anti-hepatoma activity; H22 tumor-bearing mice; Bax; Bcl-2; VEGF

Introduction

Hepatocellular carcinoma (HCC) is the fifth most prevalent tumor type and the third leading cause of cancer-related mortality worldwide [1]. Although surgical managements can cure the early stage HCC, advanced stage HCC is easy to relapse and becomes fatal [2]. Chemotherapy is one of the important methods for the treatment of tumor, but many lines of evidences showed that the antitumor activities of many chemotherapeutic agents resulted in severe side effects [3]. Recently, natural medicines with better effectiveness and lower toxicity have received more and more attentions as a potential origin of new therapeutic anti-tumor drugs for HCC patients [4, 5].

Maltol (3-hydroxy-2-methyl-4-pyrone, $C_6H_6O_3$), a naturally occurring aroma compound, is widely found in soybean, coffee, chicory, bread crusts, and caramelized foods. It is generated through maillard reaction maltose and amino acid during the heat-treatment of food (Fig. 1). Maltol is well known as the safe and reliable flavor enhancer, food preservative and natural antioxidant in the world. In addition to food field, as a metal ions chelator, maltol exhibits many practical applications in the field of catalysis, cosmetic, and pharmaceutical formulations [6, 7]. In the previous studies, it has been reported that maltol showed a strong free radical scavenging and anti-oxidative activities [8-10]. Maltol can effectively protect neuronal cells against oxidative stress-induced injury through activating NF-κB signaling pathway [11] and prevent STZ-induced diabetic kidney damage [12, 13]. Also, the results from our previous study indicated that maltol could ameliorate alcohol-induced liver injury in mice via inhibiting the oxidative stress and inflammatory response [14]. In addition, a study by Yang et al., reported that maltol could prevent the H_2O_2-induced apoptosis in human neuroblastoma

cells [15].

Insert Figure 1

Interestingly, maltol-derived organometallic complexes have potential cytotoxicity on several human cancer cell lines [16, 17]. However, up to now, the information about anti-tumor efficacy of maltol itself is quite limited. Given the potential cytotoxicity and anti-apoptosis effect of maltol on tumor cell lines *in vitro*, the present study was designed to investigate the anti-tumor efficacy of maltol in a H22 tumor-bearing mice model. To the best of our knowledge, this study is the first to demonstrate anti-tumor activity of maltol in H22 ascitic hepatocyte carcinoma transplant solid tumor model and its possible molecular mechanism.

2. Materials and Methods

2.1 Chemicals and reagents

Maltol (Purity > 99%) was bought from Reagent Factory of Shanghai Ziyi (CAS: 118-71-8, No.: ZY130419). Cyclophosphamide (CTX) was provided by Jiangsu Hengrui Pharmaceutical Co., Ltd. Hematoxylin and Eosin (H&E) dye kits were acquired from Nanjing Jiancheng Bioengineering Research Institute (Nanjing, China). Hoechst 33258 dye kit was obtained from Shanghai Beyotime Co., Ltd. (Shanghai, China). Two-site sandwich enzyme-linked immunosorbent assays (ELISA) for mouse tumor necrosis factor-α (TNF-α), interferon-γ (IFN-γ), interleukin (IL)-2, IL-6, and vascular endothelial growth factor (VEGF) were purchased from R&D systems (Minneapolis, MN, USA). Rabbit monoclonal anti-Bax, anti-Bcl-2, and anti-VEGF antibodies were purchased from Cell Signaling Technology (Danvers, MA, USA). Other chemicals were all of analytical grade from Beijing Chemical Factory.

2.2 Animals and tumor cells

Mouse hepatoma 22 ascitic tumor (H22) was obtained from Institute of Biochemistry and Cell Biology, SIBS, CAS, Shanghai, China. Murine H22 cells were maintained in the ascitic form by sequential passages into the peritoneal cavities of male ICR mice as previously described [18].

Male ICR mice, weighting 22 ~ 25 g, were obtained from the Experimental Animal Holding of Jilin University with Certificate of Quality No. of SCXK (JI) 2011-0004 (Jilin, China). The mice were kept in standard laboratory conditions with free access to diet and tap water, and acclimated to a temperature-controlled room at 23 ± 2℃ with a 12-h light/dark cycle for one week prior to use. All animals handling procedures were performed in strict accordance with the Guide for the Care and Use of Laboratory Animals (Ministry of Science and Technology of China, 2006). All experimental procedures were approved by the Ethical Committee for Laboratory Animals of Jilin Agricultural University.

2.3 Animal treatment and experimental design

After an acclimatization period of one week, murine solid tumors H22 transplanted model was established as previously described [18]. Briefly, ascites tumor cells (1×10^7 cells in 0.2 mL saline) were subcutaneously injected into the right axillary region of the mice in all groups. Twenty-four hours after inoculation, the animals were randomly divided into four groups (n = 10 per group).

Drug administration began 24 h later and treated by intragastrically injection for 15 days. The normal group and the model group animals were administrated 0.9 % normal saline intragastrically. The positive control group was treated with CTX (25.0 mg/kg/day) by

intraperitoneal injection. The groups for maltol administration intragastrically received different dosages (25 and 50 mg·kg^{-1}). The experimental design was shown in Fig. 2A.

The mice weights were recorded before and after each drug administration. 24 h after the last administration of tested drug on the 15th day of the experiment, blood samples were collected by the retrobulbar vessels and allowed to clot for 45 min at room temperature. After standing for 1 h, the serum was separated by centrifugation (1500 rpm, 10 min, and 4 °C) and stored at −20 °C for biochemical analysis. Then, all the mice were sacrificed and the whole bodies, the segregated tumor, thymus, and spleen of the mice were weighed immediately. A small piece of tissue was cut off from the tumor in each mouse and fixed in 10% buffered formalin solution (m/v) for histopathological analysis.

The tumor inhibitory rate was calculated by the following formula: tumor inhibitory rate% = (tumor weight of control group - tumor weight of tested group) / tumor weight of control group × 100%. The volume of the solid tumor was measured with a digital caliper every other day. The values obtained were calculated according to the equation: V (mm^3) $=A \times B^2/2$, where A represent the largest diameter, B represent the smallest diameter.

2.4 Survival assay

To measure the effect of maltol on survival time, thirty male ICR mice were inoculated with H22 tumor cells prepared by intraperitoneal inoculation so as to observe the mice for longer time period. The treatment was performed for 40 days and the survival time of animals was monitored and recorded daily. The test continued for 40 days and those that lived more than 40 days were defaulted as 40 days. The percent survival (%) was calculated using the following equations: percent survival (%) = [(10 − numbers of mice died in each group) /10]

× 100.

2.5 Assay of cytokines

A specific two-sided ELISA assay was performed to quantify serum levels of tumor necrosis factor-α (TNF-α), interferon-γ (IFN-γ), interleukin (IL)-2, IL-6, and vascular endothelial growth factor (VEGF) according to the manufacturer's protocols. The absorbance was measured at 450 nm in an ELISA reader (Bio-Rad, California, USA)

2.6 Hoechst 33258 staining

Hoechst 33258 staining was performed as previously described with some modifications [19]. Briefly, at the end of the experiments, the mice were euthanized and the transplanted tumor were dissected out and fixed in 10% neutral buffered formalin solution. We randomly chose three ones out of them from each group. Then, these samples were cut into 5 μm sections and stained by Hoechst 33258 (10 μg/mL). After washed by PBS for three times, stained nuclei were visualized under UV excitation and photographed under a fluorescent microscope (Olympus BX-60, Tokyo, Japan).

To quantify the fragmented and condensed staining which indicated apoptotic nucleus in the slides, we randomly chose five regions from the pictures of each tumor section. These pictures were blinded and counted by two people, and the average percentage apoptosis (%) were calculated for statistical analysis. To avoid interobserver difference, a datum is valid only if the discrepancy between these two observers is less than 10%.

2.7 H&E and TUNEL assay of tumor sections

At the end of the experiment, H22 transplanted tumor tissues were fixed in 10% neutral buffered formalin solution. The washed tumor tissues were dehydrated in descending grades

of ethanol and cleared in xylene, and then embedded in paraffin. Sections were cut at 5 μm thickness and stained with hematoxylin and eosin (H&E), then subsequently examined using a light microscope for histopathological examination.

For TUNEL assay, an in situ apoptosis detection kit (Roche Applied Science, Germany) was employed to detect apoptotic cells in the tumor sections. Briefly, the sections were treated with 20 μg/mL of proteinase K in distilled water for 10 min at room temperature. To block endogenous peroxidase, the slides were incubated in methanol containing 3% hydrogen peroxide for 20 min and sections were incubated with equilibration buffer and terminal deoxynucleotidyl transferase. Finally, the sections were incubated with anti-digoxigenin-peroxidase conjugate. Peroxidase activity in each tissue section was shown by the application of diaminobenzidine. Sections were counterstained with hematoxylin.

2.8 Immunohistochemistry

Immunohistochemical analysis was performed as previously described [20]. Briefly, the 5 μm thick paraffin sections were deparaffinized and rehydrated with a series of xylene and aqueous alcohol solutions, respectively. After antigen retrieval in citrate buffer solution (0.01 M, pH 6.0) for 20 min, the slides were washed three times with TBS (0.01 M, pH 7.4) and incubated with 1% bovine serum albumin for 1 h. The blocking serum was tapped off, and the sections were incubated in a humidified chamber at 4℃ overnight with primary antibodies against Bax (1:400), Bcl-2 (1:400) and VEGF (1:200), followed by secondary antibody for 30 min. Substrate was added to the sections for 30 min followed by DAB staining and haematoxylin counter-staining. The positive staining was determined mainly by a brownish-yellow color in the nucleus of the cells. The immunostaining intensity was analyzed by light microscopy

(Olympus BX-60, Tokyo, Japan). The immunohistochemical signal was assessed by estimating the area of the objects and the medium pixel intensity per object, as the optical density (OD). The Bax/Bcl-2 ratio is the optical density ratio of the Bax and Bcl-2 protein.

2.9. Western Blot

Equal amounts of protein (50 μg/lane) were resolved by 12 % SDS-polyacrylamide gel electrophoreses (SDS-PAGE) and transferred to polyvinylidene difluoride membranes (Millipore, MA). The membrane was further incubated with respective specific Bax (1:1000) and Bcl-2 (1:1000) antibodies. The membrane was continuously incubated with appropriate secondary antibodies coupled to horseradish peroxidase and developed in the ECL western detection reagents. The immunoreactive bands were visualized by an enhanced chemiluminescence and then were quantified by a densitometric analysis.

2.10 Statistical analysis

Statistical analysis was performed using SPSS 17.0. All values were expressed as the means ± standard derivation (S.D). The differences between experimental groups were compared by ANOVA (analysis of variance) followed by Student's *t*-test of significance where $P < 0.05$ considered to be significant. Statistical graphs were produced through GraphPad Prism 6.0.4. Image-Pro plus 6.0 was used to quantify immunohistochemical analysis and Hoechst 33258 staining.

3. Results

3.1 Effect of maltol on H22 tumor growth

The antitumor effect of maltol on H22 tumor-bearing mice is summarized in Table 1 and Fig. 2B. At the end of the experiment, the average tumor weight in the model group was 1.15 ±

0.85 g. The average tumor weights in maltol group (25 and 50 mg/kg) were decreased to 0.48 ± 0.36 and 0.42 ± 0.21 g, respectively. The average tumor weight in each maltol-treated group was dramatically lower than that of model group ($P < 0.05$). Accordingly the tumor inhibitory rates of the CTX and maltol-treated groups were 81.7, 58.2, and 63.9%, respectively.

As shown in Fig. 2B, the results from tumor volume growth curves clearly indicate that tumor volumes of the mice in model group increased rapidly during the 14 day duration with their mean volumes reaching more than 2.3 cm^3 at day 15. In contrast, the treatment of maltol and CTX significantly suppressed the tumor growth ($P < 0.05$). From the 9th day, the average tumor volume of the maltol-treated mice increased relatively slowly.

Insert Table 1

Insert Figure 2

3.2 Effect of maltol on organ indices in mice

Spleen and thymus indices, two immune parameters, are used usually to evaluate the immune function of host in H22 tumor-bearing mice. To determine whether or not maltol administration caused any side effects on the immune system, the thymus and spleen indices of the host animals were calculated at the end of the study. As shown in Table 1, the results indicated the indices of spleen and thymus in tumor-bearing mice (model) were more than those in normal mice ($P < 0.05$). Two indices in the CTX-treated mice were significantly lower than the model group ($P < 0.05$), which accounted for the immunosuppressive side effect by CTX during the therapy. However, there was no significant difference between the model group and each maltol-treated group, suggesting that maltol treatment for 14 days did not cause any side effects on the immune system.

3.3 Effect of maltol on life extension of mice

Evaluation of the effect of maltol on life extension in H22 tumor-bearing mice was accomplished and displayed in Fig. 2C. The results indicate that all of the mice in model group died within 16 days owing to the significant fast growth of H22 transplanted tumor. After treatment with CTX and maltol, half of the mice survived for more than 20 days. The average survival time of ascites H22-bearing mice treated with CTX and maltol at a dose of 50 mg/kg was 40 and 38 days, respectively. Interestingly, the survival time of mice in maltol-treated group (50 mg/kg) was almost comparable to that in CTX-treated group. The findings clearly demonstrate that maltol treatment greatly prolonged the survival period of H22 tumor-bearing mice.

3.4 Effect of maltol on the levels of serum cytokines and VEGF

To assess the effect of maltol on the production of serum cytokines such as TNF-α, IFN-γ, IL-2 and IL-6 in H22 bearing mice, we determined their serum levels by ELISA assay. As shown in Fig. 3A-D, the serum levels of TNF-α, IFN-γ, IL-2 and IL-6 in the all maltol groups were higher than that of the model group. However, only mice treated with maltol at high dose (50 mg/kg) showed significant differences ($P < 0.05$).

Angiogenesis, an essential process for tumor growth and metastasis, become an important target for therapeutic intervention in many tumors. VEGF is recognized as a key contributor to the process of angiogenesis [21]. The serum level of VEGF was determined by ELISA. As shown in Fig. 3E, the result indicate that maltol treatment at doses of 25 and 50 mg/kg markedly decreased the serum level of VEGF ($P < 0.05$, $P < 0.01$), suggesting that maltol could suppress angiogenesis in the H22 transplanted tumor.

Insert Figure 3

3.5 Morphological change by treatment of maltol

As shown in Fig. 4A, the H&E staining results indicate that tumor cells in model group were arranged tightly, having a large nucleus and clearly apparent nucleolus. However, the tumor cells in all maltol-treated groups exerted loose arrangement and a large area of necrotic region. Also, different increased degrees of vacuoles and vacuoles number were clearly observed in maltol-treated groups in a dose-dependent manner, which corroborates the remarkable anti-tumor efficacy of maltol on H22 tumor bearing mice via inducing cell death/apoptosis.

To elucidate whether maltol treatment induced cell apoptosis in H22 transplanted tumors, Hoechst 33258 staining was performed to observe apoptosis of tumor cells in this study. As depicted in Fig. 4B, we found that tumor cells in model group were observed as round-shaped nuclei with homogeneous fluorescence intensity and most cell nucleus exhibited regular contours. After treatment with maltol and CTX for 14 days, significant nuclear fragmentation and condensation was observed in dose-dependent manner.

Finally, in order to evaluate the ability of maltol treatment to induce apoptosis *in vivo*, tumor sections were stained using TUNEL colorimetric assay (Fig. 4C). This assay detects DNA fragmentation resulted from programmed cell death. The results showed that maltol treatment with 25 and 50 mg/kg caused an increase in the number of cells undergoing apoptosis compared with the model group. Similar results were obtained in tumors treated with CTX.

Insert Figure 4

3.6 Effects of maltol on expression of apoptosis-related proteins

In order to gain a better understanding of the mechanism for anti-tumor effect of maltol on H22 tumor-bearing mice, immunohistochemical analysis were performed to determine the impact of maltol on the anti-apoptotic factor Bcl-2 and the pro-apoptotic factor Bax. As depicted in Fig. 5A-B, the high expression of Bcl-2 and low expression of Bax were observed in the tumor issues section of model group. By contrast, maltol treatment decreased Bcl-2 expression and increased Bax expression of H22 tumor tissues in a dose-dependent manner. Interestingly, the ratio of Bax to Bcl-2, a rheostat of cell life or death, was increased in a dose-dependent manner after maltol treatment for 14 days ($P < 0.05$, $P < 0.01$) (Fig. 4D).

In addition, western blotting were used to analyze the anti-apoptotic factor Bcl-2 and the pro-apoptotic factor Bax. As depicted in Fig. 6, maltol treatment with 50 mg/kg increased the protein expression of Bax and inhibit the protein expression of Bcl-2 in the tumor issues section ($P < 0.05$). These results are consistent with that in immunohistochemical analysis.

Insert Figure 5

Insert Figure 6

3.7 Effects of maltol on expression of VEGF

VEGF is considered an important growth factor implicated in tumor angiogenesis and can also be used as tumor marker [21]. As shown Fig. 4C and 4E, maltol treatment could significantly inhibit the expression of VEGF in a dose-dependent manner, coinciding with the decrease of VEGF level in serum. The above observation is a hint for the possible role of maltol as angiogenesis inhibitor on H22 tumor bearing mice.

4. Discussion

To investigate the anti-tumor efficacy of maltol *in vivo*, the transplantation tumor model

was established by s.c. injection of H22 HCC cells into the right axillary region of ICR mice. Firstly, the *in vivo* anti-tumor efficacy of maltol was evaluated by the tumor growth inhibition and mice survival life prolongation rate of H22 tumor-bearing mice. The significant reduction of tumor volumes was observed in H22-bearing mice following maltol treatment at the dose of 25 and 50 mg/kg in a dose-dependent manner. The immune system plays an important role in anti-tumor defense. An increasing number of studies show that the antitumor activity of natural compounds was also mediated through augmentation of the immune response [22, 23]. In the present study, the results show that the spleen and thymus indices in all the maltol groups were comparable to model group, which clearly reveal that maltol administration could not result in any adverse effects on the immune system. Moreover, maltol treatment at dose of 50 mg/kg prolonged the survival time of tumor-bearing mice compared to model group.

Accumulating evidence clearly indicate that cytokines play a pivotal role in fighting against the tumor growth through regulating responses to affect immune cell proliferation, differentiation and functions [24]. These cytokines includes TNF-α, IL-2, IL-6, and TFN-γ. TNF- α has been proven to be an effective anticancer agent by inducing the expression of a number of other immunoregulatory and inflammatory mediators. Also, TNF-α could directly induce apoptotic cell death and tumor necrosis [25, 26]. IFN-γ is critical for innate and adaptive immunity of bacterial and anti-tumor activities [27]. In addition, several recent studies have provided powerful evidence that IL-2 and IFN-γ played an important role in specific immunological reactions to tumor cells growth, and they promoted innate and adaptive immune responses [28]. In the present study, we found that the serum levels of TNF-α, IFN-γ, IL-6 and IL-2 were significantly increased compared to model group by maltol treatment with

high dose. The considerable increase of these cytokines also explain the antitumorigenic properties of maltol. Collectively, the above findings clearly indicate the anti-tumor effect of maltol was achieved partly via increasing the immune response.

As we know, apoptosis has been characterized as a fundamental cellular activity to maintain the physiological balance of the organism [29]. As array of studies clearly demonstrate that the molecular mechanisms underlying antitumor efficacy of some chemotherapeutic agents are involved in the induction of apoptosis, which is considered to be the preferred measure to treat tumors [30]. In this study, Hoechst 33258 and TUNEL staining was performed to observe the apoptotic cells in the tumor tissues from H22 tumor-bearing mice [19]. The tumor cells in maltol treatment group showed significant cell nuclear condensation and fragmentation, which further confirmed the considerable anti-tumor activity of maltol on H22 tumor-bearing mice. Mitochondria-dependent pathway was controlled by multiple layers of regulation, the most members of the BCL-2 apoptosis-related family regulate cellular fate as a response to anticancer agents [31, 32]. There were two of the most important members concerning apoptosis in Bcl-2 family including the pro-apoptotic protein Bax and the anti-apoptotic protein Bcl-2, respectively [33]. The increase in Bcl-2 expression caused resistance to chemotherapeutic drugs and radiation therapy, while the decrease in Bcl-2 expression may promote apoptotic responses to anticancer drugs [34]. Interestingly, the relative ratio of Bax/Bcl-2, determine the sensitivity or resistance of cells to apoptotic stimuli [35]. The findings from immunohistochemistry and western blotting analysis of H22 tumor tissues show that the protein expression of Bcl-2 was significantly reduced while the protein expression of Bax was relatively increased, indicating that the maltol treatment induced

apoptosis by shifting the Bax/Bcl-2 ratio.

Numerous studies have confirmed that HCC is a highly vascular tumor and highly expresses vascular endothelial growth factor (VEGF) [36]. VEGF play a critical role in regulating tumor angiogenesis [21]. The present results showed that maltol significantly reduced the serum level of VEGF compared to the model group. Furthermore, immunohistochemical analysis verified that maltol treatment could significantly inhibit the expression of VEGF in a dose-dependent manner, coinciding with the decrease of VEGF level in serum.

In conclusion, the present work show that maltol dramatically inhibited tumor growth in transplanted ascitic H22 hepatoma mouse model. The underlying mechanisms maybe, at least in part, that maltol could improve the immune functions, induce apoptosis, and suppress angiogenesis. To the best of our knowledge, this study is the first to explore anti-tumor efficacy of maltol on H22 tumor and the possible molecular mechanism involved.

Conflicts of Interest

The authors declare no conflict of interest

Acknowledgements

This work was supported by the grants of Jilin Province Science and Technology Development Plans (NO. 20130303096YY, 20150204050YY, and 201201102), and by the grant of National Natural Science Foundation of China (NO. 31201331)

References

1. E. C. Lai and W. Y. Lau, *Surgeon*, 2005, **3**, 210-215.
2. J. Sitzia and L. Huggins, *Cancer practice*, 1998, **6**, 13-21.
3. J. Dobson, *The Veterinary record*, 2014, **174**, 248-249.
4. R. Wu, Q. Ru, L. Chen, B. Ma and C. Li, *Journal of food science*, 2014, **79**, H1430-1435.
5. L. Wang, Z. K. Nie, Q. Zhou, J. L. Zhang, J. J. Yin, W. Xu, Y. Qiu, Y. L. Ming and S. Liang, *Food & function*, 2014, **5**, 2183-2193.
6. V. Krishnakumar, D. Barathi, R. Mathammal, J. Balamani and N. Jayamani, *Spectrochim Acta A Mol Biomol Spectrosc*, 2014, **121**, 245-253.
7. A. Anwar-Mohamed and A. O. El-Kadi, *Toxicol In Vitro*, 2007, **21**, 685-690.
8. K. G. Lee and T. Shibamoto, *J Agric Food Chem*, 2000, **48**, 4290-4293.
9. A. Wei, K. Mura and T. Shibamoto, *Journal of agricultural and food chemistry*, 2001, **49**, 4097-4101.
10. K. G. Lee, A. Mitchell and T. Shibamoto, *BioFactors*, 2000, **13**, 173-178.
11. S. Hong, Y. Iizuka, T. Lee, C. Y. Kim and G. J. Seong, *Molecular vision*, 2014, **20**, 1456-1462.
12. K. S. Kang, N. Yamabe, H. Y. Kim and T. Yokozawa, *J Pharm Pharmacol*, 2008, **60**, 445-452.
13. K. S. Kang, H. Y. Kim, N. Yamabe, R. Nagai and T. Yokozawa, *Biological & pharmaceutical bulletin*, 2006, **29**, 1678-1684.
14. Y. Han, Q. Xu, J. N. Hu, X. Y. Han, W. Li and L. C. Zhao, *Nutrients*, 2015, **7**, 682-696.
15. Y. Yang, J. Wang, C. Xu, H. Pan and Z. Zhang, *Journal of biochemistry and molecular biology*, 2006, **39**, 145-149.
16. O. Domotor, S. Aicher, M. Schmidlehner, M. S. Novak, A. Roller, M. A. Jakupec, W. Kandioller, C. G. Hartinger, B. K. Keppler and E. A. Enyedy, *J Inorg Biochem*, 2014, **134**, 57-65.
17. W. Kandioller, C. G. Hartinger, A. A. Nazarov, C. Bartel, M. Skocic, M. A. Jakupec, V. B. Arion and B. K. Keppler, *Chemistry*, 2009, **15**, 12283-12291.
18. J. Yang, X. Li, Y. Xue, N. Wang and W. Liu, *International journal of biological macromolecules*, 2014, **64**, 276-280.
19. X. Zhao, G. Shu, L. Chen, X. Mi, Z. Mei and X. Deng, *Food and chemical toxicology : an international journal published for the British Industrial Biological Research Association*, 2012, **50**, 3166-3173.
20. W. Cheng, L. Miao, H. Zhang, O. Yang, H. Ge, Y. Li and L. Wang, *Digestive and liver disease : official journal of the Italian Society of Gastroenterology and the Italian Association for the Study of the Liver*, 2013, **45**, 50-57.
21. B. Liu, H. Zhang, J. Li, C. Lu, G. Chen, G. Zhang, A. Lu and X. He, *Planta medica*, 2013, **79**, 1401-1407.
22. A. Zhang, Y. Zheng, Z. Que, L. Zhang, S. Lin, V. Le, J. Liu and J. Tian, *Journal of cancer research and clinical oncology*, 2014, **140**, 1883-1890.
23. M. C. Bibby, R. M. Phillips, J. A. Double and G. Pratesi, *British journal of cancer*, 1991, **63**, 57-62.
24. C. Chen, V. E. Cowles, M. Sweeney, I. D. Stolyarov and S. N. Illarioshkin, *Clin Neuropharmacol*, 2012, **35**, 67-72.
25. R. S. Rajmani, P. K. Singh, G. Ravi Kumar, S. Saxena, L. V. Singh, R. Kumar, A. P. Sahoo, S. K. Gupta, U. Chaturvedi and A. K. Tiwari, *Anim Biotechnol*, 2015, **26**, 112-119.
26. F. J. Lejeune, D. Lienard, M. Matter and C. Ruegg, *Cancer Immun*, 2006, **6**, 6.
27. B. Gansbacher, R. Bannerji, B. Daniels, K. Zier, K. Cronin and E. Gilboa, *Cancer Res*, 1990, **50**, 7820-7825.
28. G. Wang, J. Zhao, J. Liu, Y. Huang, J. J. Zhong and W. Tang, *Int Immunopharmacol*, 2007, **7**, 864-870.

29. Y. L. Hsu, P. L. Kuo, C. F. Liu and C. C. Lin, *Cancer Lett*, 2004, **212**, 53-60.
30. J. M. Brown and B. G. Wouters, *Cancer Res*, 1999, **59**, 1391-1399.
31. V. Gogvadze, S. Orrenius and B. Zhivotovsky, *Biochim Biophys Acta*, 2006, **1757**, 639-647.
32. C. K. Kontos, M. I. Christodoulou and A. Scorilas, *Anti-cancer agents in medicinal chemistry*, 2014, **14**, 353-374.
33. I. M. Ghobrial, T. E. Witzig and A. A. Adjei, *CA Cancer J Clin*, 2005, **55**, 178-194.
34. C. Gapany, M. Zhao and A. Zimmermann, *J Hepatol*, 1997, **26**, 535-542.
35. J. T. Li, J. L. Zhang, H. He, Z. L. Ma, Z. K. Nie, Z. Z. Wang and X. G. Xu, *Food and chemical toxicology : an international journal published for the British Industrial Biological Research Association*, 2013, **51**, 297-305.
36. F. Yang, J. Li, J. Zhu, D. Wang, S. Chen and X. Bai, *European journal of pharmacology*, 2015, **754**, 105-114.

Figure legends

Figure 1. Formation pathway of maltol in maillard reaction between maltose and amino acid.

Figure 2. Experiment design scheme (A). Effects of maltol on tumor growth (B) and life extension in H22 tumor-bearing mice (C).

Figure 3. Effects of maltol on the levels of serum TNF-α (A), IFN-γ (B), IL-2 (C), IL-6 (D), and VEGF (E) in H22 tumor-bearing mice. All data were expressed as mean ± S.D, n= 10. $^{*}P < 0.05$, $^{**}P < 0.01$ *vs* model group.

Figure 4. Histological examination of morphological changes in tumors from H22-bearing mice. Tumor tissues stained with H&E (100×) (A) and Hoechst 33258 (100×) (B-C). Tumor sections were analyzed by TUNEL assay to indicate cell apoptosis (D). The images were analyzed by an Image-Pro plus system. The necrosis and apoptosis of tumor cells were marked by arrow heads. All data were expressed as mean ± S.D. $^{*}P < 0.05$, $^{**}P < 0.01$ *vs* model group.

Figure 5. Effects of maltol on the expression of Bax, Bcl-2, and VEGF (A-E). The protein expression was examined by immunohistochemistry. The images were analyzed by an Image-Pro plus system. All data were expressed as mean ± S.D. $^{*}P < 0.05$, $^{**}P < 0.01$ *vs* model group.

Figure 6. Relative protein expression of Bax and Bcl-2 in tumor tissues. All data were expressed as mean ± S.D. $^{*}P < 0.05$, *vs* model group.

Table 1. Effects of maltol on tumor weights and relative organ indices in H22 tumor-bearing mice.

Groups	Dosage (mg/kg)	Organ indices (mg/g)		Tumor weight (g)	Inhibitory rate (%)
		Spleen	Thymus		
Normal	—	0.37±0.07	0.11±0.01	—	—
Model	—	0.69±0.27$^{\#}$	0.24±0.11$^{\#}$	1.15±0.85	—
CTX	25	0.41±0.07*	0.13±0.01*	0.21±0.12**	81.7%
Maltol	25	0.62±0.16	0.22±0.04	0.48±0.36*	58.2%
	50	0.68±0.07	0.23±0.03	0.42±0.21*	63.9%

Values are expressed as the mean ± S.D, $n = 10$. $^{\#}$ $P < 0.05$ *vs* normal group * $P < 0.05$, ** $P < 0.01$ *vs* model group

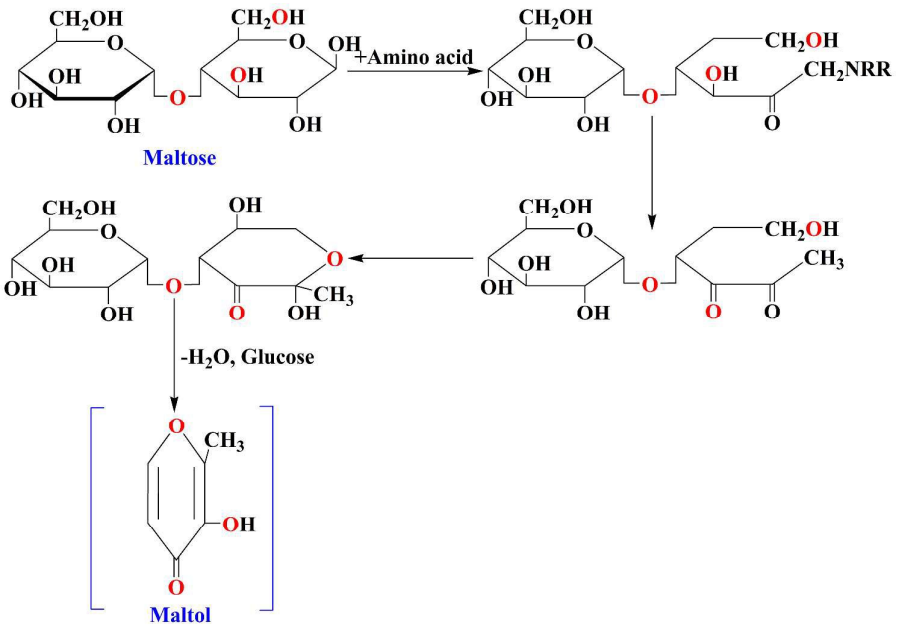

Figure 1

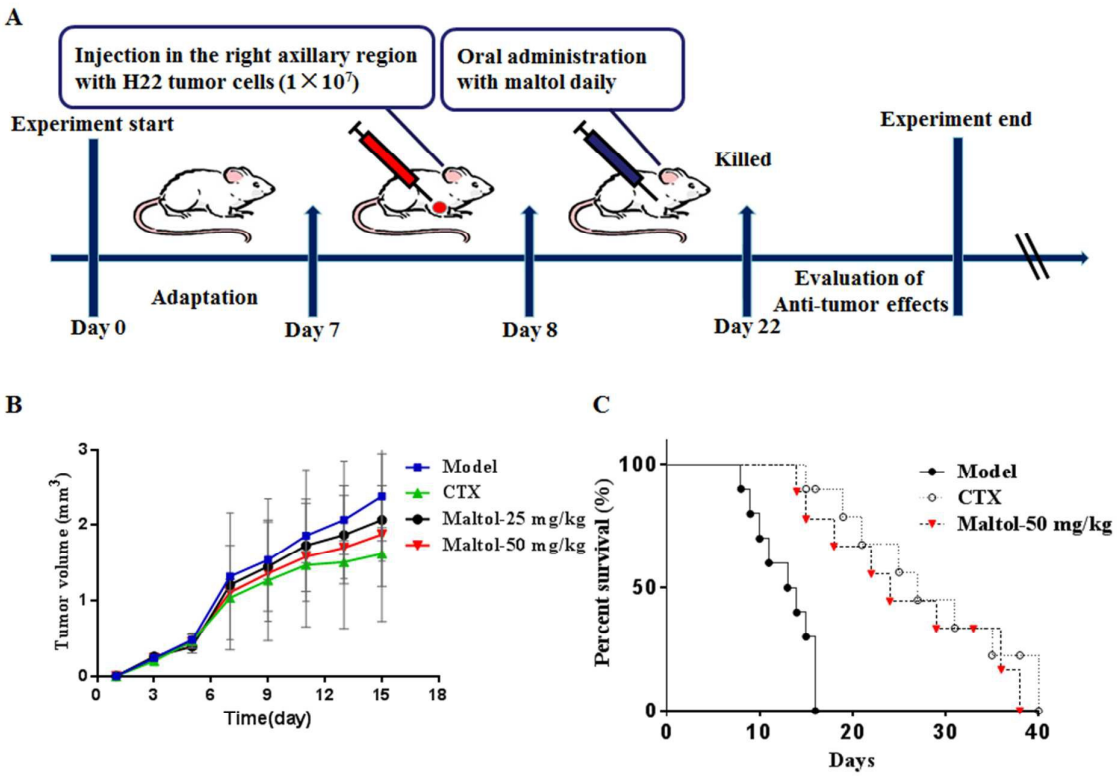

Figure 2

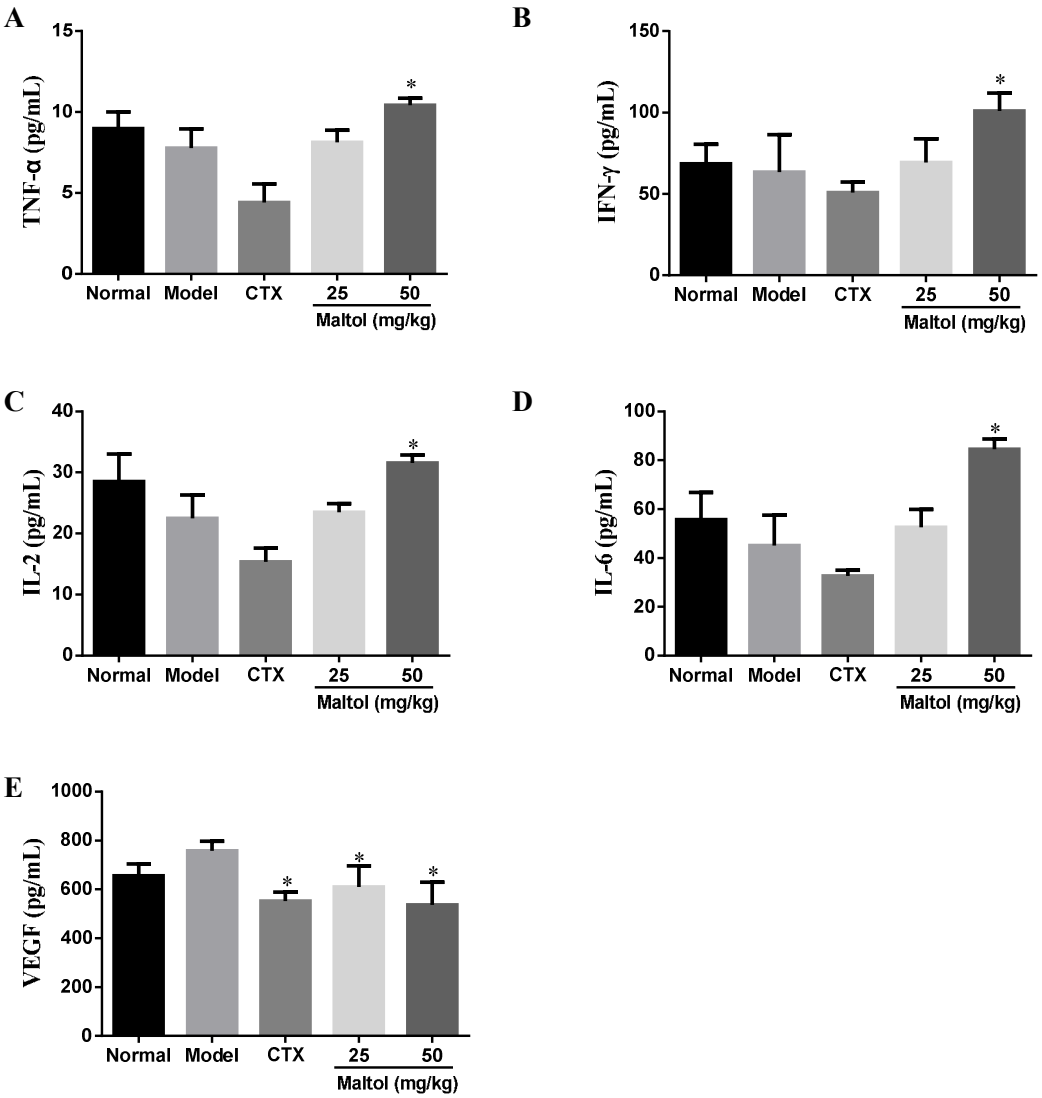

Figure 3

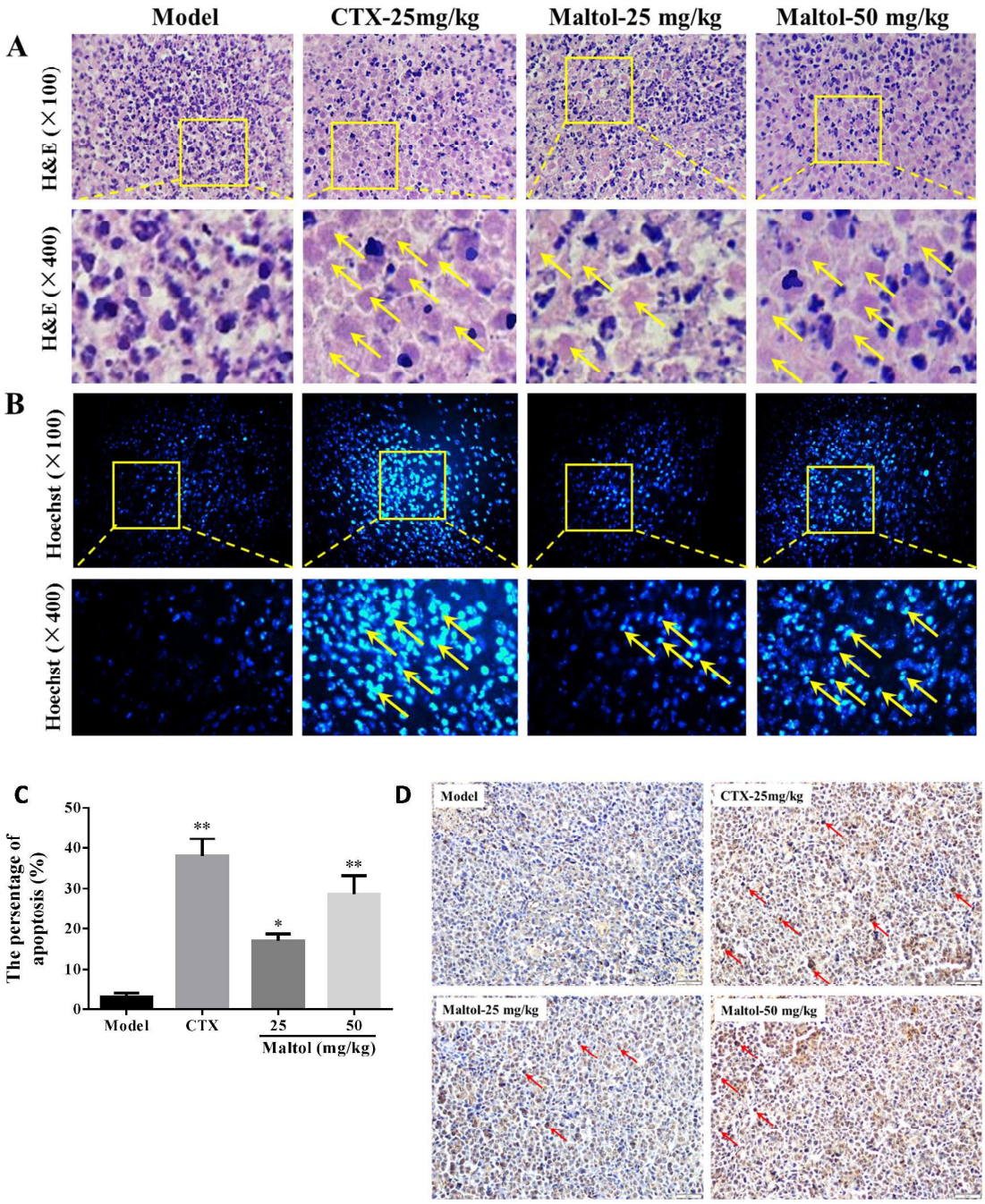

Figure 4

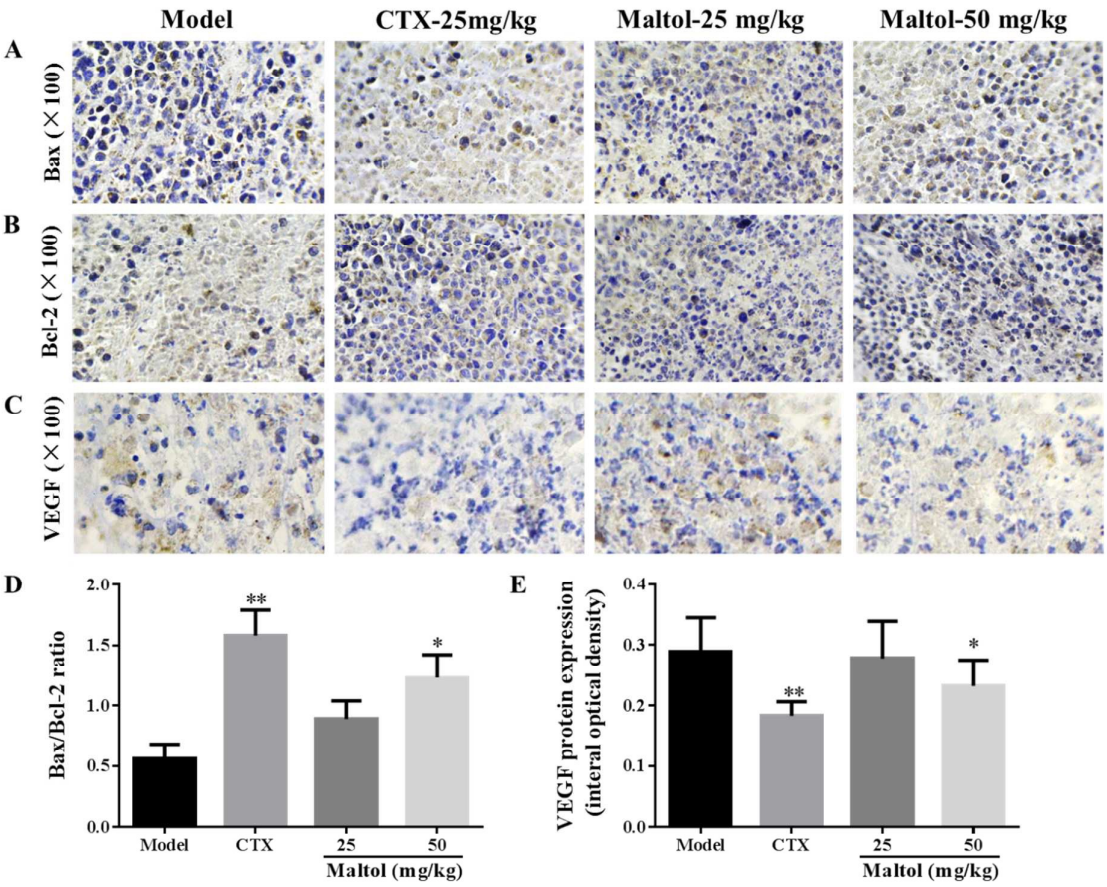

Figure 5

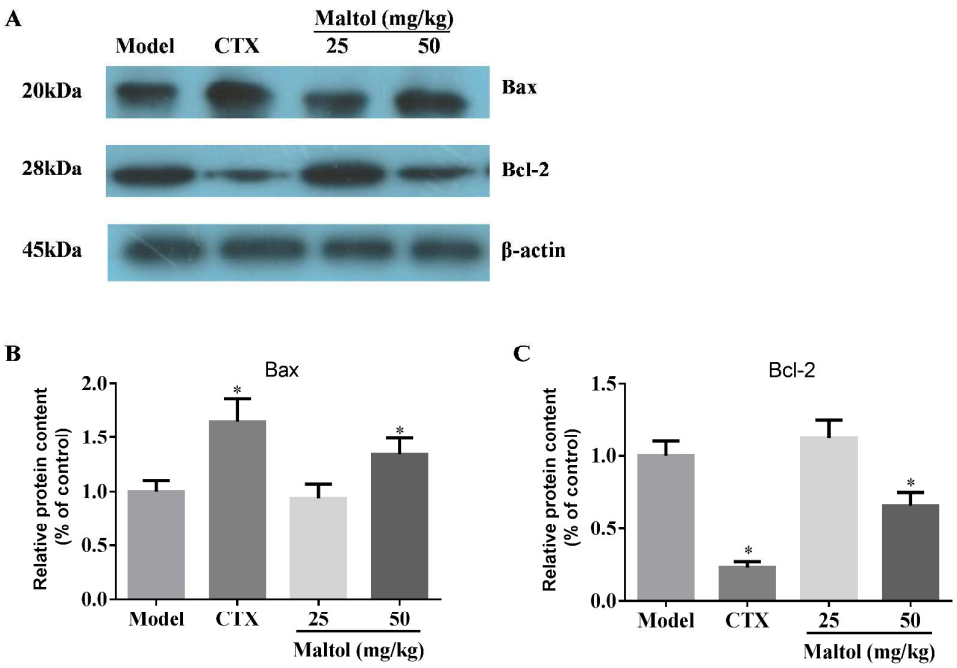

Figure 6